Effects of Incident Beam Points on Optical Heterodyne Detection of Gaussian Plane Waves

Ichiro SAKURABA* and Teruhito MISHIMA*

(Received April 30, 1970)

Contents

Abstract

The effect of incident beam points on optical heterodyne detection of Gaussian plane waves was presented. The derivation was based on Corcoran and Sakuraba's analysis for a one-dimensional photocathode.

The full width for the power pattern between half-power points decreases when the distribution length increases in the case where the cathode width and the wavelength are kept constant and the signal and local-oscillator beams are assumed to be directed toward the middle point of the cathode width. A chart which shows the effect of incident beam points on the full width of 3-db points is given.

1. Introduction

Angular selectivity properties of uniform plane waves in optical heterodyne detection have been pointed out by Siegman, Harris, and McMurtry[1], Corcoran[2], Stroke[3] and Siegman[4]. DeLange has shown a curve of effect of beam tilt in Gaussian plane waves on output current[5]. The directional characteristics of two-dimensional photocathodes has been shown by Sakuraba and Tsubo[6]. The wavefront curvature effect on detected power output has recently been given by Sakuraba[7] and the fundamental properties of Gaussian plane wave in optical heterodyne detectors have more recently been shown by the present authors[8][9].

The purpose of this paper is to derive the directional characteristics of Gaussian plane waves in optical heterodyne detection when the signal and local-oscillator beams are assumed to be directed towards their respective incident points on the photocathode.

2. Detected Power Output

A schematic representation of the problem of a combination of Gaussian plane waves incident on a photocathode is shown in Fig. 1. The photocathode is a strip of width L in the z-direction and uniform in the x-direction. The local-oscillator beam is assumed to be directied towards a point z_{01} on the cathode at an angle of

* Department of Electronic Engineering. Faculty of Engineering, Hokkaido University, Sapporo, Japan

incidence θ_1 and the signal beam is assumed to be directed towards a point z_{02} on the photocathode at an angle of incidence θ_2. When the field at P on the detector

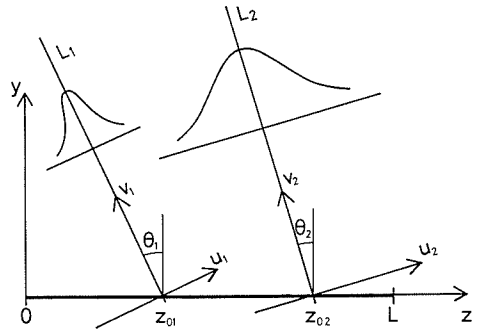

Fig. 1. Schematic diagram showing the illumination of the cathode by Gaussian plane waves.

surface is due to the superposition of two waves, the ac output current of the detector can be expressed as

$$i(t) = e^{-j(\omega_1-\omega_2)t}\int_A E_1(P)E_2^*(P)\,dA\,, \tag{1}$$

where ω_1 and ω_2 are optical frequencies, $E_1(P)$ and $E_2(P)$ are components of the electric field at P on the cathode and A is the photosensitive area[2),7)]. The unessential constant factor was dropped and the angular brackets which indicate a time average over an interval were ignored. It was assumed that the two beams have the same optical modes and they are identically polarized. It is conventional to relate the peak ac photocurrent i_1 to the power output through a fictitious equivalent resistance R_{eq} defined by the equation[1),10)]

$$P_{out} = \frac{1}{2}|i_1|^2 R_{eq}\,. \tag{2}$$

The equivalent resistance depends on the circuit characteristics of the optical devices and its output connections. From Eqs. (1) and (2) the expression for the output can be written as

$$P_{out} = \frac{1}{2}R_{eq}\left|\int_A E_1(P)\cdot E_2^*(P)dA\right|^2 \tag{3}$$

The fields at $P(0, 0, z)$ on the detection surface are given by

$$E_1(P) = A_1 \exp\left[-(u_1/u_{01})^2 - jk_1v_1\right], \tag{4}$$

and

$$E_2(P) = A_2 \exp\left[-(u_1/u_{02})^2 - jk_2v_2\right], \tag{5}$$

where A_1 and A_2 are complex constants, k_1 and k_2 are propagation constants and u_{01} and u_{02} are amplitude distribution lengths (see Appendix). By geometry as shown in Fig. 1:

$$v_1 = y\cos\theta_1 - (z-z_{01})\sin\theta_1\,, \tag{6}$$

$$u_1 = (z-z_{01})\cos\theta_1 + y\sin\theta_1 , \tag{7}$$

$$v_2 = y\cos\theta_2 - (z-z_{02})\sin\theta_2 , \tag{8}$$

$$u_2 = (z-z_{02})\cos\theta_2 + y\sin\theta_2 , \tag{9}$$

and

$$\theta_1, \theta_2 \neq \pi/2 . \tag{10}$$

By substitution in Eqs. (4) and (5), we obtain

$$E_1(z) = E_1(P)|_{y=0} = A_1 \exp\left[-jk_1 z_{01}\sin\theta_1 - \left(\frac{z-z_{01}}{u_{01}/\cos\theta_1}\right)^2 + jk_1 z\sin\theta_1\right], \tag{11}$$

$$E_2(z) = E_2(P)|_{y=0} = A_2 \exp\left[-jk_2 z_{02}\sin\theta_2 - \left(\frac{z-z_{02}}{u_{02}/\cos\theta_2}\right)^2 + jk_2 z\sin\theta^2\right], \tag{12}$$

and

$$P_{\text{out}} = \frac{1}{2} R_{\text{eq}} |A_1 A_2^*|^2 \times \left| \int_0^L \exp\left[-\frac{(z-\alpha)^2}{\gamma^2} - \frac{(z_{01}-z_{02})^2}{(u_{01}/\cos\theta_1)^2 + (u_{02}/\cos\theta_2)^2} - j\beta_c z \right] dz \right|^2 , \tag{13}$$

where

$$\alpha = \frac{z_{01}(u_{02}/\cos\theta_2)^2 + z_{02}(u_{01}/\cos\theta_1)^2}{(u_{01}/\cos\theta_1)^2 + (u_{02}/\cos\theta_2)^2} , \tag{14}$$

$$\beta_c = k_2\sin\theta_2 - k_1\sin\theta_1 , \tag{15}$$

and

$$\gamma^2 = \frac{(u_{01}/\cos\theta_1)^2 (u_{02}/\cos\theta_2)^2}{(u_{01}/\cos\theta_1)^2 + (u_{02}/\cos\theta_2)^2} . \tag{16}$$

By putting

$$\xi = z/L , \quad \xi_{01} = z_{01}/L , \quad \xi_{02} = z_{02}/L , \tag{17}$$

$$w_{01} = u_{01}/L\cos\theta_1 , \quad w_{02} = u_{02}/L\cos\theta_2 , \tag{18}$$

$$l_1 = \lambda_1/L\sin\theta_1 , \quad l_2 = \lambda_2/L\sin\theta_2 , \tag{19}$$

and

$$k_{1z} = k_1\sin\theta_1 , \quad k_{2z} = k_2\sin\theta_2 , \tag{20}$$

the power output may be rewritten as

$$P_{\text{out}} = \frac{1}{2} R_{\text{eq}} |A_1 A_2^*|^2 L^2 \left| \int_0^1 \exp\left[\frac{-(\xi-a)^2}{g^2} - \frac{(\xi_{01}-\xi_{02})^2}{w_{01}^2 + w_{02}^2} - jb\xi \right] d\xi \right|^2 \tag{21}$$

where

$$a = \frac{\xi_{01} w_{02}^2 + \xi_{02} w_{01}^2}{w_{01}^2 + w_{02}^2} , \tag{22}$$

$$b = (k_{1z} - k_{2z})L , \tag{23}$$

$$g^2 = \frac{w_{01}^2 w_{02}^2}{w_{01}^2 + w_{02}^2}. \tag{24}$$

The quantities of w_{01} and w_{02} are normalized amplitude distribution lengths in the x-direction and the quantities of l_1 and l_2 are normalized lengths between two points

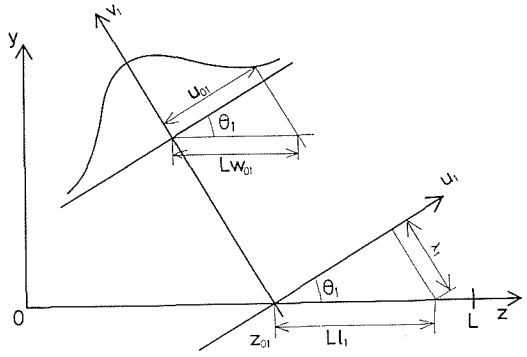

Fig. 2. Relation between θ_1, u_{01}, w_{01}, l_1, λ_1 and L.

which have the phase difference of 2π on the detector surface (see Fig. 2). The x-components of the propagation constants are k_{1x} and k_{2x}.

Now consider two special cases of interest. The first special case is that in which we let w_{01} and w_{02} approach infinity. Then Eq. (21) becomes

$$P_{\text{out}} = (R_{\text{eq}}/2)|A_1 A_2^*|^2 L^2 D_g^2, \tag{25}$$

$$D_g^2 = \text{sinc}^2(b/2). \tag{26}$$

where the notation sinc $x=(\sin x)/x$ is used. This is nothing but the directivity factor of optical heterodyne detection of uniform plane waves[1),6)7)]. In the case where two beams are nearly equal and are at non-normal angles, $\theta_1=\theta$ and $\theta_2=\theta+\delta\theta$, the full width of the main lobe measured from half-power point to half-power point on either side of the beam direction $2B=2\delta\theta$, becomes

$$2B = 0.888\,\lambda/L\cos\theta, \tag{27}$$

where λ is the optical wavelength and it was assumed that $\lambda_1 \approx \lambda_2 = \lambda$.

The second special case of interest is that in which the two light beams are assumed to be directed towards a point $z_{01}=z_{02}=z_{0x}$ on the photocathode and the length of distribution on the cathode is small compared with the cathode length. Thus Eq. (21) becomes

$$P_{\text{out}} = (\pi R_{\text{eq}}/2)|A_1 A_2^*|^2 g^2 L^2 D_g^2, \tag{28}$$

$$D_g^2 = \exp(-b^2 g^2/2). \tag{29}$$

The quantity mentioned above D_g specifies the normalized directivity factor in heterodyning of Gaussian plane waves[8)]. In the case where $\theta_1=\theta$ and $\theta_2=\theta+\delta\theta$, the full width for the power pattern between half-power or 3-db points is

$$2B = 0.375\,\lambda\sqrt{\left(\frac{1}{u_{01}}\right)^2 + \left(\frac{1}{u_{02}}\right)^2} \tag{30}$$

It should be noted that this equation does not include the incident angle θ.

3. Examples and Discussion

When $w_{01}=w_{02}=w_{0n}$, $\xi_{01}=\xi_{02}=0.5$, $\theta_1=0$, $\theta_2=\delta\theta$, $L=2$ mm and $\lambda=0.633\,\mu$, the power pattern with $\delta\theta$ for various values of w_{0n} is plotted in Fig. 3. The pattern is normalized to a value of power output in the case of exactly parallel incidence. As the distribution length increases, the parameter w_{0n} increases and the width of the main lobe becomes narrower and side lobes appear and finally they approach the power pattern of optical heterodyne detection of uniform plane waves. The first zero in the pattern for $w_{0n}=0.5$ occurs at $\theta_2=\delta\theta=5.3\times10^{-4}$ rad. The first side lobe for $w_{0n}=0.5$ is 36.7 db down from the peak value of main lobe at $\delta\theta=5.9\times10^{-4}$ rad and the second lobe is 31.9 *db* down. The first zero for $w_{0n}=2.0$ is at $\theta_2=\delta\theta=3.3\times10^{-4}$

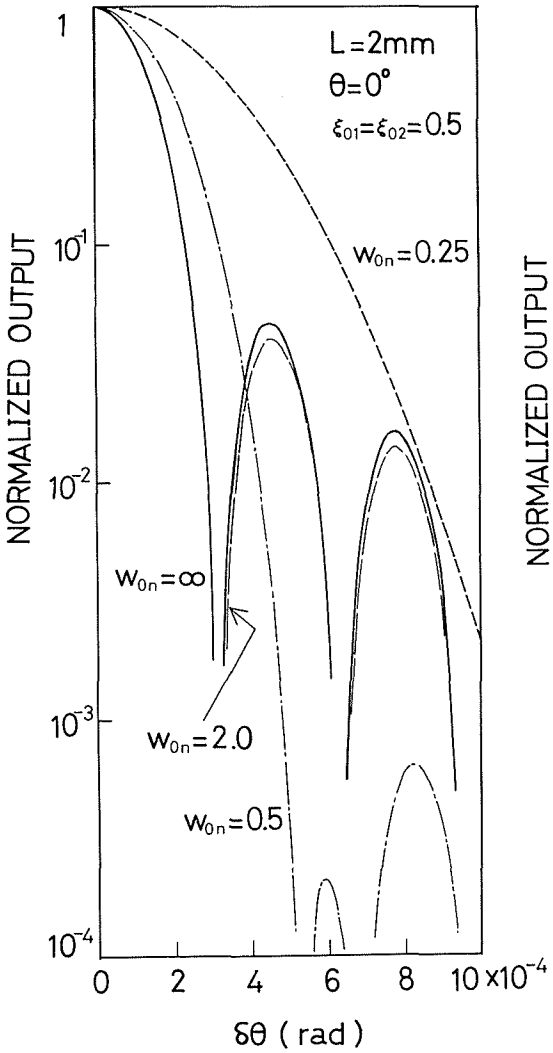

Fig. 3. The calculated normalized output vs. $\delta\theta$ with w_{0n} as the parameter in the case where $\theta_1=0$, $\theta_2=\delta\theta$, $L=2$ mm and $\xi_{01}=\xi_{02}=0.5$ at 0.633 μ.

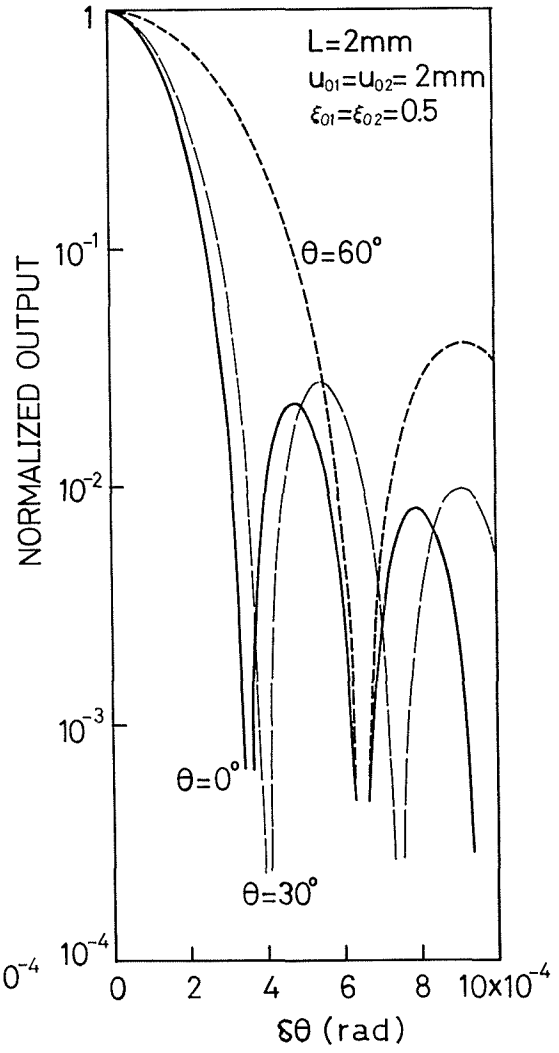

Fig. 4. The calculated normalized output vs. $\delta\theta$ with θ as the parameter in the case where $\theta_1=\theta$, $\theta_2=\theta+\delta\theta$, $L=2$ mm, $u_{01}=u_{02}=2$ mm and $\xi_{01}=\xi_{02}=0.5$ at 0.633 μ.

rad and the first side lobe is 14.0 db down from the peak at $\delta\theta = 4.55 \times 10^{-4}$ rad and the second is 18.6 db down. The power pattern for uniform plane waves, $w_{0n} = \infty$, is also shown in Fig. 3. A study of Fig. 3 shows that the patterns for $w_{0n} > 2.0$ and $w_{0n} = \infty$ are almost the same.

Plots of the normalized output as function $\delta\theta$ for various values of θ are presented in Fig. 4, when $u_{01} = u_{02} = 2$ mm, $L = 2$ mm, $\xi_{01} = \xi_{02} = 0.5$, $\theta_1 = \theta$, $\theta_2 = \theta + \delta\theta$ at 0.633 μ. As the value of incident angle increases and the distribution length is kept constant, the directivity decreases. Namely, the directional pattern of nearly equal and non-normal angles is less sensitive to angles than that of normal incidence and non-parallel beams, as was expected. Because, it is considered that the factors which influence the directivity are the parameters w_{0n} and z-components of propagation constants when the incident beam angle is changed. As it is clear from Eq. (27) and results of Corcoran[2] and Siegman[4], the power pattern of uniform plane waves also shows a similar tendency.

Plots of normalized output with cathode length as the parameter are shown in Fig. 5. It was assumed that $u_{01} = u_{02} = 2$ mm, $\theta_1 = 0$, $\theta_2 = \delta\theta$ and $\xi_{01} = \xi_{02} = 0.5$. Figure

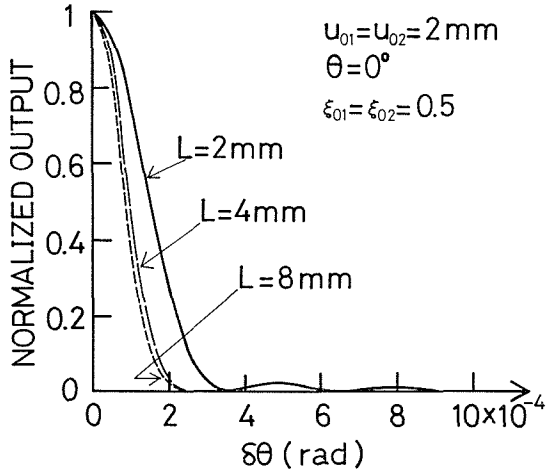

Fig. 5. The calculated normalized output vs. $\delta\theta$ with L as the parameter in the case in which $\theta_1 = 0$, $\theta_2 = \delta\theta$, $u_{01} = u_{02} = 2$ mm, and $\xi_{01} = \xi_{02} = 0.5$ at 0.633 μ.

5 shows that the directional pattern is narrowed as the cathode width increase in the case of constant distribution length and the factors affecting the directivity could be parameters of w_{0n} and z-components of propagation constants.

Now consider examples of effects of incident beam points on the directivity. Figures 6, 7, and 8 show the normalized outpt with ξ_{02} as the parameter in the case where $\xi_{01} = 0$, 0.25, and 0.5, respectively, when $L = 2$ mm, $u_{01} = u_{02} = 1$ mm, $\theta_1 = 0$ and $\theta_2 = \delta\theta$ at 0.633 μ. These results show that when we replace the value of ξ_{01} with that of ξ_{02} in the case where $w_{01} = w_{02}$, the power pattern remains the same. In the case in which $\xi_{01} = \xi_{02} = 0.5$ many side lobes appear and they have numerous zero points in the pattern and they do not necessarily have zero points in the other case.

When $L = 2$ mm, $u_{01} = u_{02} = 5$ mm, $\theta_1 = 0$, $\theta_2 = \delta\theta$ at 0.633 μ, the power pattern for $\xi_{01} = 0$ and $1 \geqq \xi_{02} \geqq 0$ are given in Fig. 9. As seen from this Figure, the effects of values of ξ_{02}, namely the incident point of signal beam, can be neglected and there

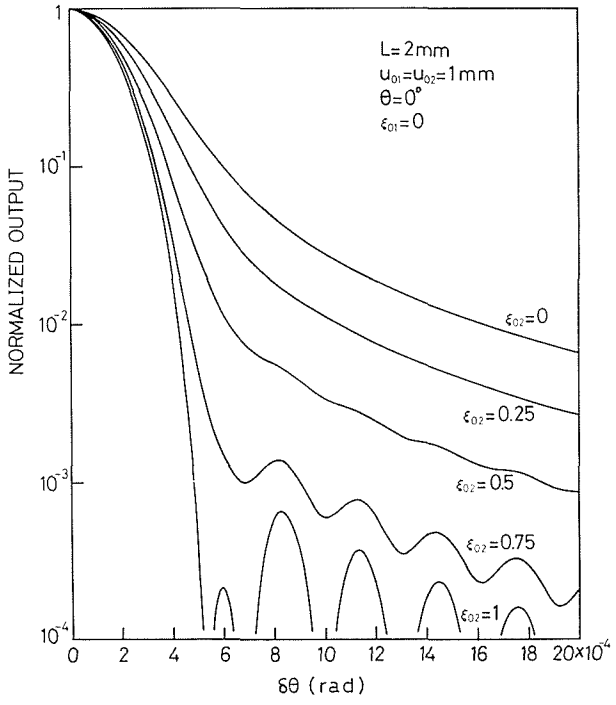

Fig. 6. The calculated normalized output vs. $\delta\theta$ with ξ_{02} as the parameter in the case where $\theta_1=0$, $\theta_2=\delta\theta$, $L=2$ mm, $u_{01}=u_{02}=1$ mm and $\xi_{01}=0$ at 0.633 μ.

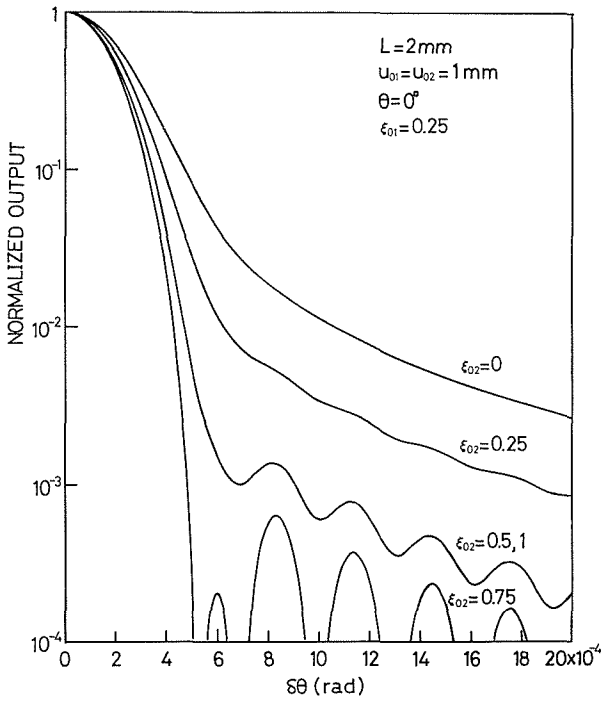

Fig. 7. The calculated normalized output vs. $\delta\theta$ with ξ_{02} as the parameter in the case in which $\theta_1=0$, $\theta_2=\delta\theta$, $L=2$ mm, $u_{01}=u_{02}=1$ mm and $\xi_{01}=0.25$ at 0.633 μ.

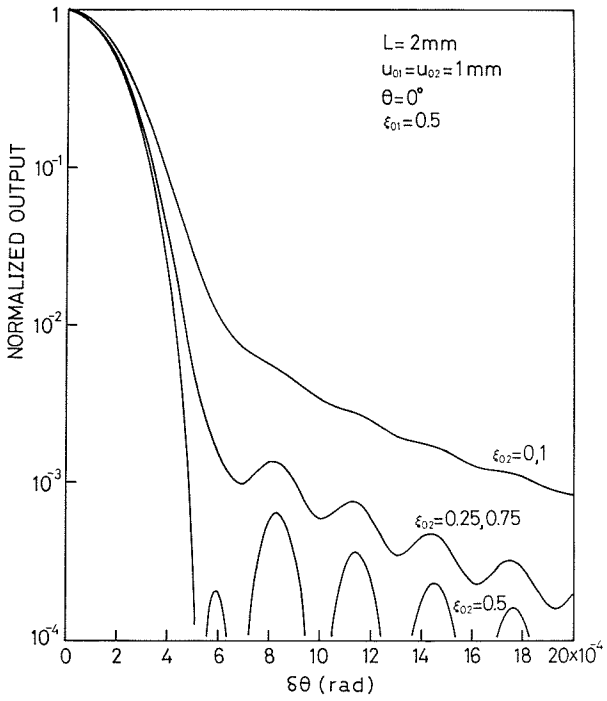

Fig. 8. The calculated normalized output vs. $\delta\theta$ with ξ_{02} as the parameter in the case where $\theta_1=0$, $\theta_2=\delta\theta$, $L=2$ mm, $u_{01}=u_{02}=1$ mm and $\xi_{01}=0.5$ at 0.633 μ.

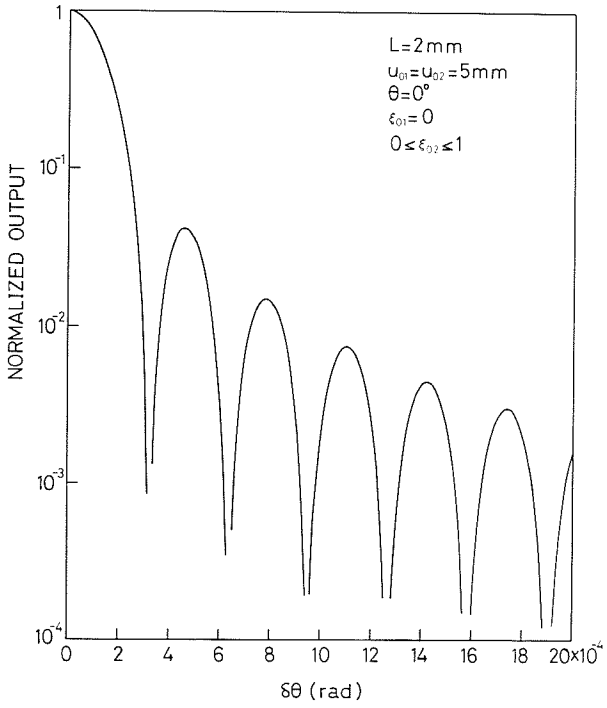

Fig. 9. The calculated normalized output vs. $\delta\theta$ in the case in which $\theta_1=0$, $\theta_2=\delta\theta$, $L=2$ mm, $u_{01}=u_{02}=5$ mm, $\xi_{01}=0$ and $0\leqq\xi_{02}\leqq1$ at 0.633 μ.

is not appreciable change in power patterns as $w_{01}=w_{02}>2.5$, $\xi_{01}=0$ and constant values of L, $u_{01}=u_{02}$ and $\theta_1=0$.

When $L=2$ mm, $\theta_1=0$, $\theta_2=\delta\theta$, $w_{01}=w_{02}=w_{0n}$, and $\xi_{01}=\xi_{02}=0.5$ at 0.633 μ, the full width for the power pattern between half-power points was solved on the digital computer with Eq. (21) and the calculation points are shown in Fig. 10. Also shown

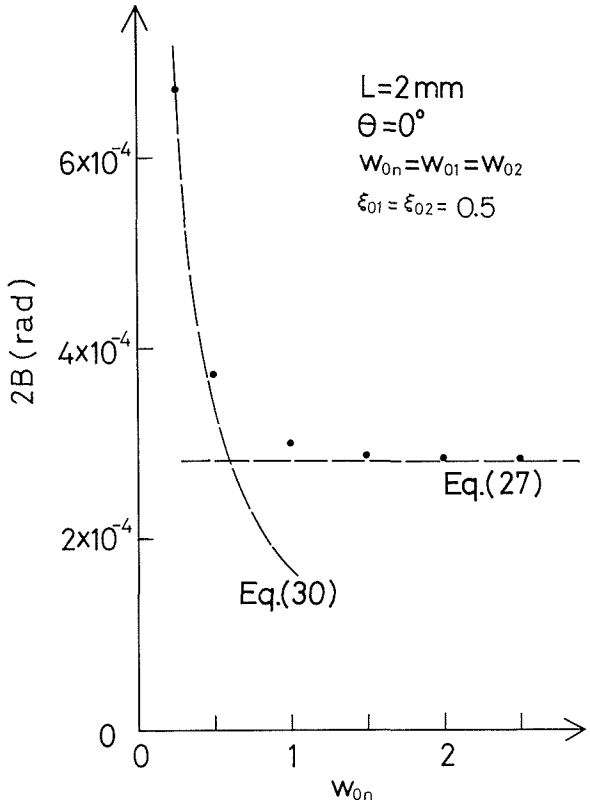

Fig. 10. The full width between 3-db points vs. w_{0n} in the case where $\theta_1=0$, $\theta_2=\delta\theta$, $w_{01}=w_{02}=w_{0n}$, $L=2$ mm, $\xi_{01}=\xi_{02}=0.5$ at 0.633 μ. The full width for uniform plane waves and for Gaussian plane waves of very small distribution lengths are also shown. They are obtained from Eqs. (27) and (30), respectively.

in this Figure are the full widths between 3-db points for the uniform plane waves and the Gaussian plane waves of very small distribution lengths obtained from Eqs. (27) and (30). The correlation is seen to be close enough at the small w_{0n} end and the large w_{0n} end.

The full widths between 3-db points in the case of nearly equal and non-normal angles are presented in Fig. 11, by assuming that $L=2$ mm, $w_{01}=w_{02}=w_{0n}$, $\xi_{01}=\xi_{02}=0.5$, $\theta_1=\theta$, $\theta_2=\theta+\delta\theta$ and $\lambda=0.633$ μ. The calculation points were obtained from Eq. (21) in a typical case of θ as $u_{01}=u_{02}=1$ mm and 2 mm. Plots of Eqs. (27) and (30) under the same condition are also shown in this Figure. In the case where $u_{01}=u_{02}=2$ mm, calculation values obtained from Eq. (21) agree well with the theoretical results of uniform plane wave determined from Eq. (27) so that it can be considered that there is no effect of distribution lengths, but it is logical that some

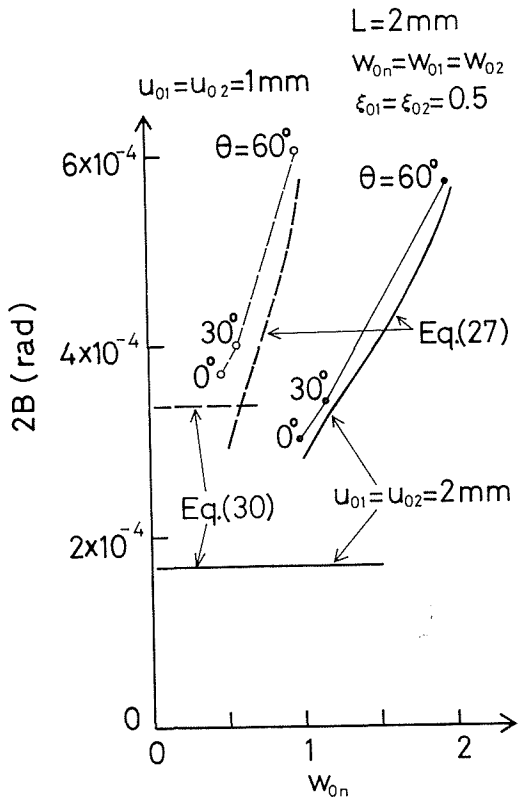

Fig. 11. The full width between 3-db points vs. w_{0n} with θ as the parameter in the case in which $\theta_1=\theta$, $\theta_2=\theta+\delta\theta$, $L=2$ mm, $w_{01}=w_{02}=w_{0n}$ and $\xi_{01}=\xi_{02}=0.5$ at 0.633 μ. The curve for $u_{01}=u_{02}=2$ mm are shown by a solid line and for $u_{01}=u_{02}=1$ mm, by a broken line. Eqs. (27) and (30) show the full widths of uniform plane waves and Gaussian plane waves of very small distribution lengths, respectively.

difference between results of Eqs. (21) and (30) arises. In the case in which $u_{01}=u_{02}=1$ mm as shown by the broken line the difference at small values of w_{0n} becomes small and calculated values from Eq. (21) approximately agree with the result of Eq. (27). It shoud be emphasized that the factors which influence the full width between 3-db points are w_{0n} and z-components of propagation constants as the incidents angle is changed. Figure 12 shows the full width between half-points vs. ξ_{01} and ξ_{02} with $u_{01}=u_{02}$ as the parameter when $L=2$ mm, $\theta_1=0$ and $\theta_2=\delta\theta$ at 0.633 μ. The effect of incident beam points on the full width of 3-db points can be easily obtained from this chart.

4. Conclusions

The effects of incident beam points on optical heterodyne detection of Gaussian plane waves were investigated. The general characteristics may be summarized as follows:

1) When the distribution length increases in the case in which $\theta_1=0$, $\theta_2=\delta\theta$, $\xi_{01}=\xi_{02}=0.5$ and the cathode width and the wavelength are kept constant, the width of

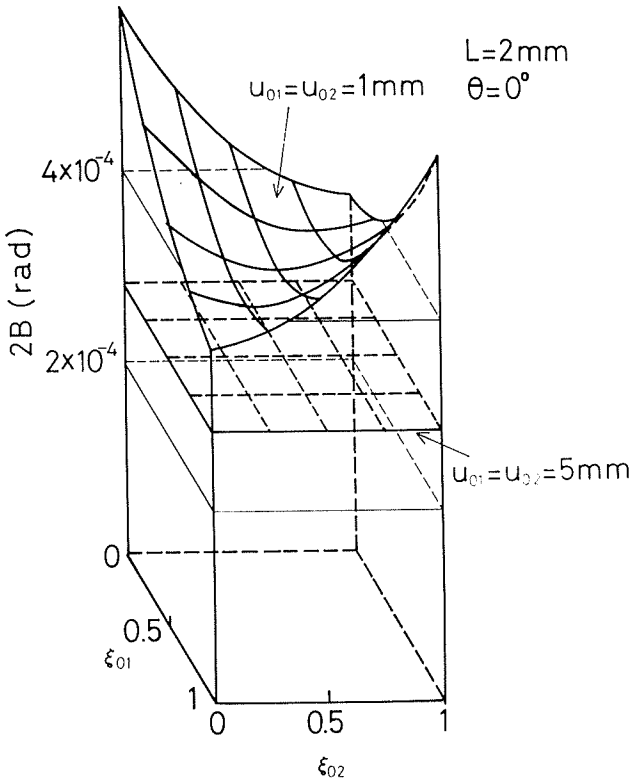

Fig. 12. The full width vs. ξ_{01} and ξ_{02} with $u_{01}=u_{02}$ as the parameter. It was assumed that $L=2$ mm, $\theta_1=0$, and $\theta_2=\delta\theta$ at 0.633 μ.

main lobe becomes narrowed and side lobes appear and finally they approach the power pattern of optical heterodyne detection of uniform plane waves.

2) In the case where $\theta_2=\theta$, $\theta_2=\theta+\delta\theta$, $\xi_{01}=\xi_{02}=0.5$ and the distribution length, the cathode width and the wavelength are kept constant, the directional pattern of nearly equal and non-normal angles is less sensitive than that of normal incidence and non-parallel beams.

3) When the cathode width increases in the case in which $\theta_1=0$, $\theta_2=\delta\theta$, $\xi_{01}=\xi_{02}=0.5$ and the distribution length and the wave length are kept constant, the directional pattern is narrowed.

4) In the case where $\theta_1=0$, $\theta_2=\delta\theta$, and the cathode width, the distribution length and the wavelength are kept constant, the power pattern remains the same as we replace the value of ξ_{01} with that of ξ_{02} in the same normalized amplitude distribution length. The power pattern for $\xi_{01}=\xi_{02}=0.5$ has numerous zero points and in the other case of ξ_{01} and ξ_{02} it does not necessarily have zero points.

5) In the case in which $\theta_1=0$, $\theta_2=\delta\theta$, $w_{01}=w_{02}>2.5$ and the wavelength is kept constant, there is not appreciable change in power patterns and the effect of incident beam points can be neglected.

6) When the distribution length increases in the case where $\theta_1=0$, $\theta_2=\delta\theta$, $\xi_{01}=\xi_{02}=0.5$ and the cathode width and the wavelength are kept constant, the full width between 3-db points decreases. The full width for large w_{0n} can be given by Eq. (27) and the width for very small w_{0n} can be shown by Eq. (30). The effect of incident beam points on the full width of 3-db points is shown in Fig. 12.

7) When the incident angle increases in the case where $\theta_1=\theta$, $\theta_2=\theta+\delta\theta$, $\xi_{01}=\xi_{02}=0.5$ and the cathode width, the wavelength and the distribution length are kept constant, the full width between 3-db points increases. This tendency is the same as the full width of uniform plane waves.

Acknowledgment

The authors are greatly indebted to the Staff of the Research Institute of Applied Electricity, Hokkaido University, for making computer time avaiable for this study. Also, the authors wish to thank Mr. K. Koyanagi and Mr. H. Takajō for their helpful suggestions. Finally, we are grateful to Professor M. Suzuki for his helpful observations and critical reading of the manuscrtpt.

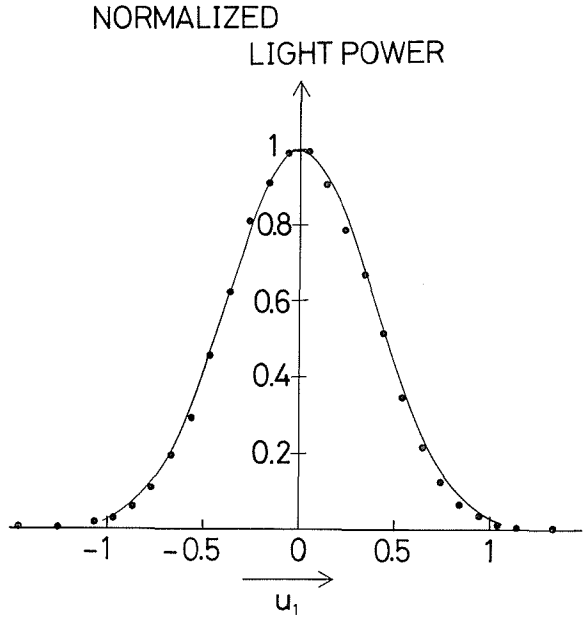

Fig. A-1. Typical distribution of laser beam. The theoretical value is given by a solid line and the points show experimental values.

Appendix

The experimental values of laser-beam distribution are given in Fig. A-1. The laser used in this work was a 6328 Å and single-mode He-Ne laser and the power was detected by a photomultiplier. The distribution length was 0.753 mm and theoretical curve whose distribution length has the same value was also shown in this Figure.

References

1) Siegman, A. E., Harris, S. E., and McMurtry, B. J.: "Optical heterodyning and optical demodulation at microwave frequencies", Proc. Symp. on Optical Maser, Polytechnic Institute of Brooklyn, New York, pp. 511-527, April 1963.
2) Corcoran, V. J.: "Directional characteristics in optical heterodyne detection processes", J. Appl. Phys,. vol. 36, pp. 1819-1825, June, 1965.

3) Stroke, G. W.: Lectures on "Optics of coherent and non-coherent electromagnetic radiations" Department of Electrical Engineering, The University of Michigan, Ann Arbor, Michigan, 1964 and J. Opt. Soc. Am., vol. 47, pp. 1097–1103, 1957.
4) Siegman, A. E.: "The antenna properties of optical heterodyne detection receiver", Proc. IEEE, vol. 54, pp. 1350–1356, October 1966.
5) DeLange, O. E.: "Optical Heterodyne Detection", IEEE Spectrum, vol. 5, pp. 77–85, October 1968.
6) Sakuraba, I. and Tsubo, T.: "Directional characteristics and forms of the detector surface in optical heterodyne detection processes", Memoirs of the Faculty of Engineering, Hokkaido University, Sapporo, Japan, No. 56, pp. 295–318, January 1969.
7) Sakuraba, I.: "Signal power output and wavefront curvature in optical heterodyne detection processes", Memoirs of the Faculty of Engineering, Hokkaido University, Sapporo, Japan, No. 57, pp. 417–426, February 1970.
8) Sakuraba, I.: "Directional characteristics of Gaussian plane waves in optical heterodyne detection", Memoirs of Faculty of Engineering, Hokkaido University, Sapporo, Japan, No. 57, pp. 427–438, February 1970.
9) Sakuraba, I. and Mishima, T.: "Directional characteristics of Gaussian plane waves in optical heterodyne detection", Proc. IEEE, to be published.
10) Sakuraba, I. and Rowe, J. E.: "Partial conversion of current modulation in linear-photoelectron-beam systems", Trans. PTGED-IEEE, vol. ED-12, pp. 388–389, June 1965.